frontiers | Frontiers in Materials

TYPE Original Research
PUBLISHED 18 January 2024
DOI 10.3389/fmats.2024.1354635

OPEN ACCESS

EDITED BY
Veerappan Mani,
King Abdullah University of Science and Technology, Saudi Arabia

REVIEWED BY
Abdellatif Ait Lahcen,
Cornell University, United States
Zhengao Wang,
South China University of Technology, China

*CORRESPONDENCE
Cheng Wang,
wangcheng98@126.com
Xiaogang Zhao,
zhaoxgthoracic@163.com

†These authors have contributed equally to this work

RECEIVED 12 December 2023
ACCEPTED 08 January 2024
PUBLISHED 18 January 2024

CITATION
Zhang Y, Shen C, Tang Y, Li X, Liu D, Wei A, Wang C and Zhao X (2024), CNT-doped transition metal carbide enables sensitive organic electrochemical transistor based carcinoembryonic antigen aptasensor towards precise lung cancer diagnosis. *Front. Mater.* 11:1354635. doi: 10.3389/fmats.2024.1354635

CNT-doped transition metal carbide enables sensitive organic electrochemical transistor based carcinoembryonic antigen aptasensor towards precise lung cancer diagnosis

Yunzeng Zhang[1,2,3]†, Changming Shen[3]†, Yan Tang[4], Xiaofeng Li[3], Dawei Liu[3], Ailin Wei[5], Cheng Wang[3]* and Xiaogang Zhao[1,2]*

[1]School of Medicine, Shandong University, Jinan, Shandong, China, [2]Department of Thoracic Surgery, The Second Hospital of Shandong University, Jinan, Shandong, China, [3]Department of Thoracic Surgery, Shandong Public Health Clinical Center, Shandong University, Jinan, Shandong, China, [4]Department of Respiratory and Critical Care, Shandong Public Health Clinical Center, Shandong University, Jinan, Shandong, China, [5]Department of Scientific Management, Guang'an People's Hospital, Guang'an, Sichuan, China

Effective detection of carcinoembryonic antigen (CEA) plays an important role in the diagnosis of lung cancer. Given the challenges posed by the low abundance and complexity of biosamples, it is urgent to develop sensitive, cost-effective and fast detection strategies. In this paper, a novel platform is developed using doped transition metal carbides as semiconductor materials for organic electrochemical transistor (OECT) aptamer-based sensors to satisfy sensitivity, specificity, rapidity, and low cost. A new material, CNT-doped MXene, was synthesized and utilized in the fabrication of CM-OECATs. The morphology and doping of CNT-doped MXene were validated effectively. 2.0 wt% CNT achieved maximum doping efficiency at transconductance (Gm) of 0.801 ms. Through systematic optimization of temperature, pH, aptamer concentration and incubation time, a wide detection range ranging from 0.1 pg/mL to 100 ng/mL was achieved, and the lower limit was 0.051 pg/mL. Favorable stability (0.819% decline), specificity and repeatability (RSD = 2.05%) were demonstrated. CM-OECATs effectively distinguished between 11 biosamples of lung cancer from 12 healthy controls (AUC = 0.9748, specificity = 0.9565, sensitivity = 0.9978) for the clinics. The test carried out in two batches gave p-values <0.05, indicating the effectiveness of the CM-OECATs in discriminating effectively. In addition, CM-OECATs demonstrated a favourable correlation in 25 clinical samples ($y = 0.9782x + 0.7532$, $R^2 = 0.9723$). To sum up, an organic electrochemical transistor aptamer-based sensor based on CNT-doped MXene (CM-OECATs) is promising for future real-time monitoring in clinical settings, paving the way for an efficient, cost-effective and highly sensitive detection strategy.

KEYWORDS

CNTs-doped MXene, organic electrochemical transistor, carcinoembryonic antigen, aptamer, lung cancer

1 Introduction

The paramount importance of early detection and precise identification in lung cancer diagnosis can't be overstated (Yang et al., 2019; Sung et al., 2021; Wang et al., 2022), as it enables timely and effective therapeutic interventions, thereby enhancing patient survival rates and overall quality of life. However, diagnosing lung cancer poses challenges due to subtle early symptoms, which are often overlooked, and the current lack of highly sensitive, real-time, and cost-effective detection methods (Wang et al., 2019; Huang et al., 2022). Consequently, there is a pressing need for innovative technologies to augment diagnostic accuracy and efficiency. Carcinoembryonic antigen (CEA), as a biomarker for lung cancer, emerges as a pivotal indicator owing to its elevated presence in lung cancer patients (Paniagua et al., 2019; Qiu et al., 2019; Chen et al., 2023). Therefore, devising effective strategies for the efficient detection of CEA is crucial for improving lung cancer diagnosis.

In comparison to methods such as plasma chips, enzyme-linked immunosorbent assay (ELISA), and Surface-enhanced Raman Spectroscopy, organic electrochemical transistors (OECTs) offer distinct advantages, including low cost, rapidity, and real-time detection capabilities (Ramuz et al., 2015; Moser et al., 2020; Spyropoulos et al., 2020; Guo K. et al., 2021a). The fundamental principle encompasses the amplification of tiny signal perturbations via semiconductor materials for detection, imposing unique requirements on these materials. Transition metal carbides (MXene), with their favourable semiconductor properties and unique defect structures facilitating carrier migration and doping (Qin et al., 2018; Zhang et al., 2020; Wang et al., 2021; Zahed et al., 2022), represent a novel sensor material with a large specific surface area crucial for active site interaction. Carbon nanotubes, known for their favourable conductivity, are widely used to enhance the sensitivity of electrochemical sensors (Wee et al., 2010; Wei et al., 2022; Zamzami et al., 2022). However, the utilization of carbon nanotube-doped MXene for CEA detection has not been reported.

This study addressed this gap by applying carbon nanotube-doped MXene in transistor biosensors, coupled with CEA aptamers, to construct an aptamer sensor (CNT-doped MXene-based organic electrochemical aptasensor transistor, CM-OECATs) for specific CEA detection in lung cancer diagnosis (Figure 1A). We systematically verified the structure and morphology of carbon nanotube-doped MXene and optimized the pH, temperature, aptamer concentration, and incubation time of CM-OECATs sensors. As a result, CM-OECATs demonstrated acceptable performance in stability (0.819% decline), specificity, and reproducibility (RSD = 2.05%). By utilizing CNT-doped MXene as the organic electrochemical transistor material and leveraging the double electrical layer effect (Figures 1B, C), the sensor achieved detection within the range of 0.1 pg/mL-100 ng/mL, with a low detection limit of 0.051 pg/mL. In clinical sample analysis, CM-OECATs effectively differentiated 11 lung cancer serum samples from 12 healthy control samples (AUC = 0.9748, Specificity = 0.9565, Sensitivity = 0.9978). *t*-test results for two sample batches yielded a *p*-value of 0.0064 < 0.05, indicating effective discrimination by CM-OECATs. In 25 clinical samples, CM-OECATs demonstrated favourable clinical correlation with the target values (y = 0.9782x + 0.7532, R^2 = 0.9723). In summary, the organic electrochemical transistor aptamer sensor (CM-OECATs) constructed based on CNT-doped MXene holds promise for future real-time clinical monitoring, paving the way for efficient, low-cost, and highly sensitive detection technologies.

2 Materials and methods

2.1 Synthesis of CNT-doped MXene

The synthesis process of CNT-doped MXene begins with a reaction between 1 g of Ti_3AlC_2 and 3 mL of 2 M sodium hydroxide solution, left to react overnight for 12 h (Mojtabavi et al., 2019; Mojtabavi et al., 2019; Kim et al., 2021). This results in the formation of MXene material with a two-dimensional structure. Subsequently, centrifugation and drying are performed to obtain powdered MXene. Different concentrations of carbon nanotubes (Chengdu Organic Chemistry Ltd.) are then subjected to a hydrothermal reaction with MXene powder at mass fractions of 1.0%, 2.0%, and 3.0%. The specific reaction parameters entail a comprehensive reaction between MXene and carbon nanotubes at 80°C (López Barreiro et al., 2019; Wang et al., 2021; Guo et al., 2022). The resulting products are used in the fabrication of CM-OECATs.

2.2 Preparation of CM-OECATs

To prepare CM-OECATs, a semiconductor material with various ratios of CNT-doped MXene is first synthesized at a concentration of 1 g/mL. Subsequently, it is spin-coated onto a screen-printed electrode at 1000 RPM for 120 s. After achieving uniformity, the electrode is dried on a heating plate at 90°C for 5 min. Plasma cleaning of the working electrode is then performed for 3 min (Li et al., 2017; Meirinho et al., 2017; Wang et al., 2020), followed by 12 h of binding with a CEA aptamer with a sequence of SH-ATACCAGCTTATTCAATT (Si et al., 2017). After sufficient binding, the electrode is blocked using 20 μM mercaptoacetic acid for 6 h. The final CM-OECATs are stored in a refrigerated environment at 4°C.

2.3 Characterization

Scanning electron microscopy is carried out using the FlexSEM 1000 II, while transmission electron microscopy is performed using the Thermo Fisher Talos L120C. Transfer curves are measured using a Keithley 2612B.

2.4 Collection and analysis of clinical samples

Serum samples from patients or healthy individuals are collected, centrifuged at 1,200 g for 5 min, and finally sealed and stored at −20°C. Receiver Operating Characteristic (ROC) analysis, t-tests, and correlation curves are processed using SPSS software.

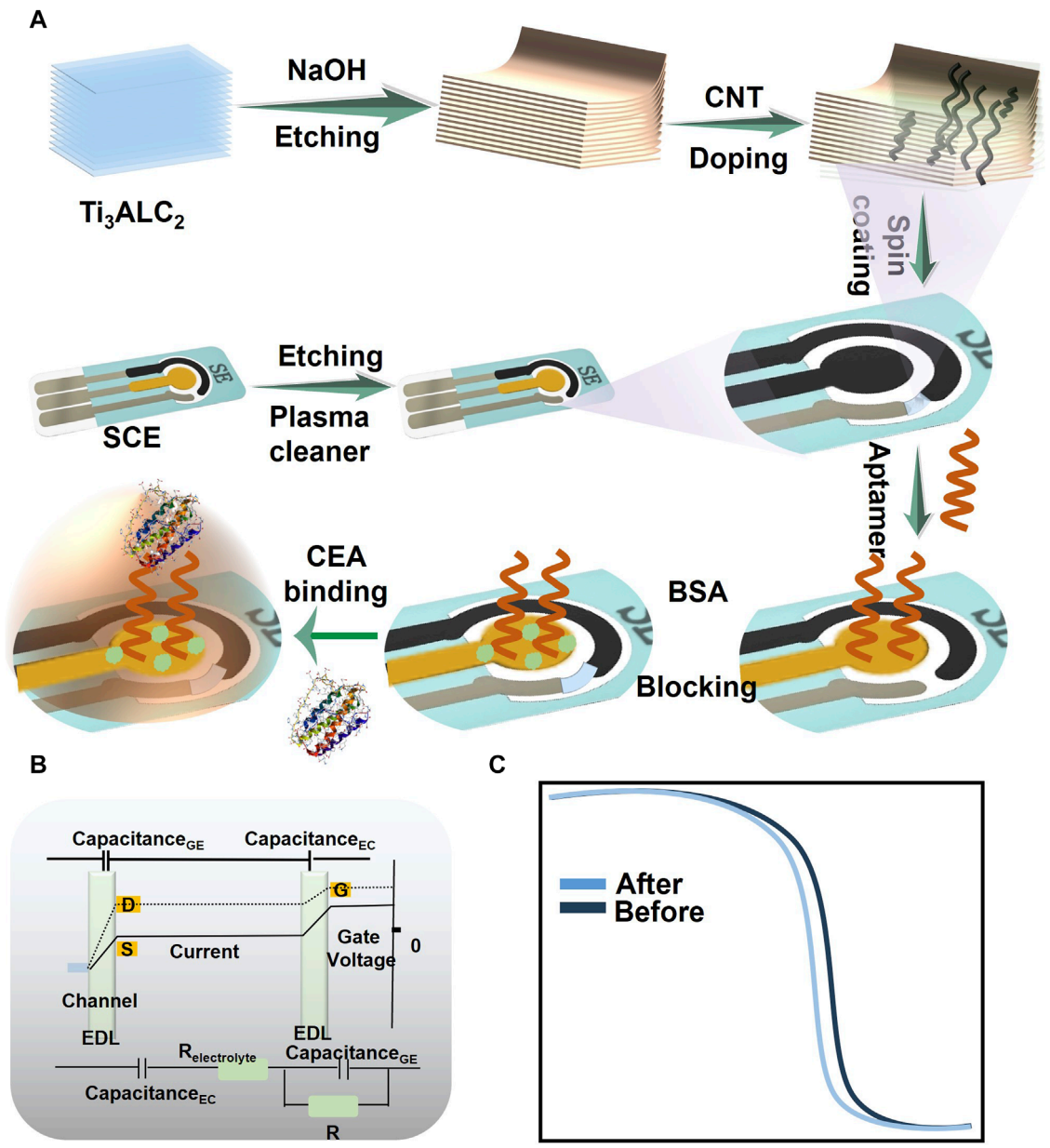

FIGURE 1
Schematic diagram illustrating the principle of CEA detection by CM-OECATs. **(A)** Preparation process of CM-OECATs, including CNT-doped MXene preparation, sensor fabrication, and functionalization steps. **(B)** Amplification of small signals through the dual capacitance effect of OECTs. **(C)** Transfer curves of CM-OECATs before and after binding with CEA.

3 Results

3.1 Characterizations of CM-OECATs

Taking into account the considerable impact of the semiconductor material composition and morphology on OECT sensors, we incorporated CNT into MXene material to modulate the semiconductor performance of the sensor. Scanning electron microscopy and transmission electron microscopy images of carbon nanotubes demonstrate their morphology (Figures 2A, B). Subsequently, we obtained MXene material with a unique layered structure through sodium hydroxide etching of transition metal carbides (Figure 2C). Additionally, we employed a hydrothermal synthesis method to combine CNT with MXene, as characterized by SEM (Figure 2D). High-resolution transmission electron microscopy and selected area electron diffraction (SEAD) analysis of CNT-doped MXene revealed a unique lattice structure (0.256 nm, Figure 2E) and distinct diffraction rings related to its hexagonal crystal structure (Figure 2F), consistent with literature reports (Hui et al., 2019; Guo Y. et al., 2021b). The above verification of morphology and hybridization effectively establishes a beneficial foundation for the next steps in CM-OECATs.

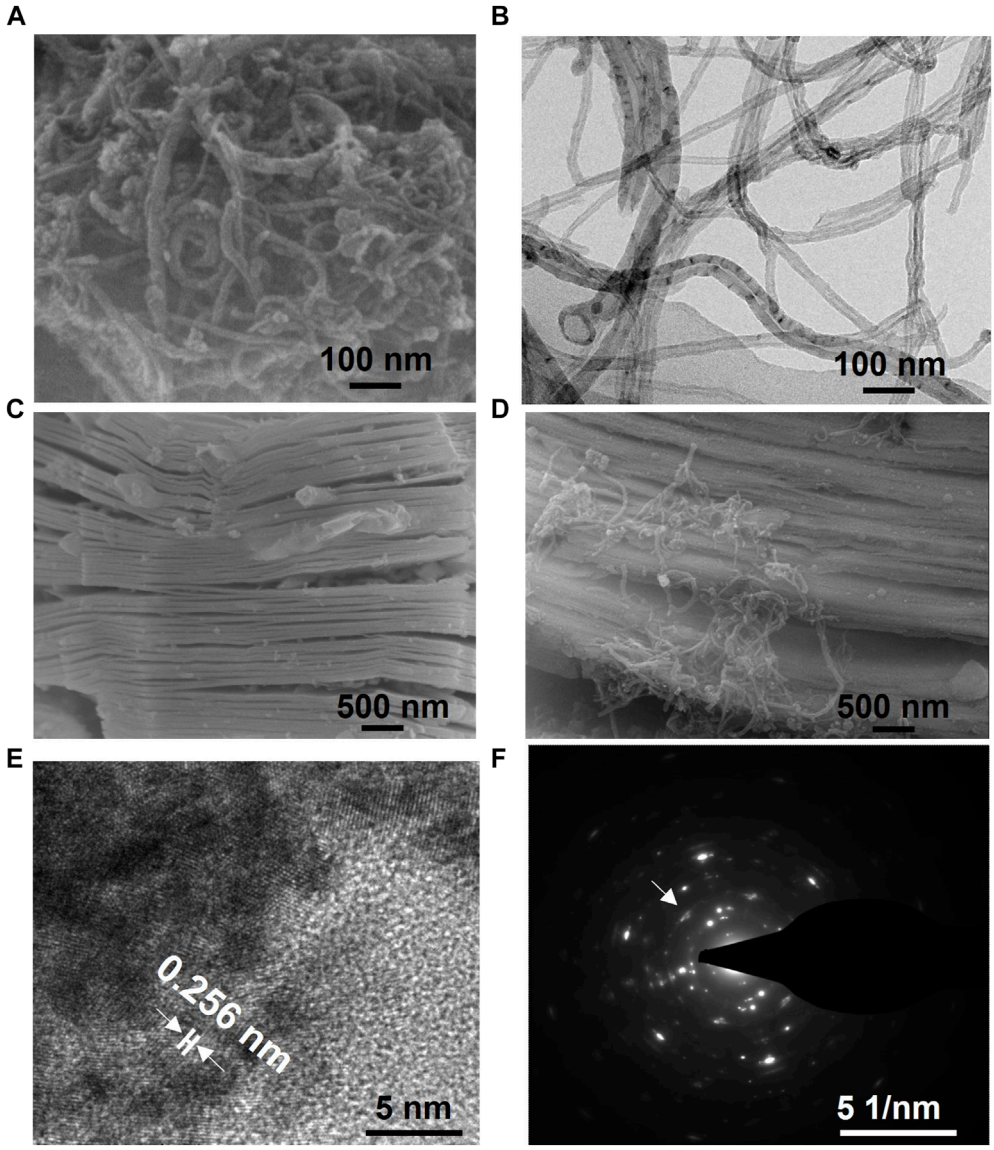

FIGURE 2
Characterizations of CM-OECATs. **(A)** Scanning electron microscopy image and **(B)** transmission electron microscopy image of carbon nanotubes. **(C)** Scanning electron microscopy image of MXene and **(D)** CNT-doped MXene. Carbon nanotubes effectively adhere to the surface of MXene, enhancing its semiconductor and conductive properties, thereby improving the detection performance of CM-OECATs. **(E)** High-resolution transmission electron microscopy image and **(F)** SEAD image of CNT-doped MXene.

3.2 Optimizations of CM-OECATs

To evaluate the influence of carbon nanotube doping on CM-OECATs, we used transconductance (G_m) to compare its different effects (Wu et al., 2019; Wu et al., 2019). Transconductance represents the level at which CM-OECATs amplify small signals. For different carbon nanotube concentrations, the transconductance of CNT-doped MXene showed an upward trend followed by a decline, reaching a maximum of 0.801 mS at a carbon nanotube proportion of 2.0 wt% (Figure 3A). This phenomenon could be attributed to the initial enhancement of CNT-doped MXene conductivity with the increasing carbon nanotube concentration. However, excessively high CNT concentration reduces the carrier migration efficiency of CNT-doped MXene, leading to a plateau in transconductance (Supplementary Table S1, Eq. 1). This also indicates that the appropriate dopant concentration is crucial for effectively promoting the semiconductor performance of MXene. Simultaneously, we optimized important parameters such as aptamer concentration, time, pH, and temperature. Transconductance curves before and after CM-OECATs binding with CEA for parameter evaluation are shown in Figure 3B. Regarding aptamer concentration optimization, the maximum value for the CM-OECATs aptamer sensor is attained at approximately 20 μM (9.12 ± 0.68 μA, Figure 3C). Regarding aptamer incubation time, the incubation time for

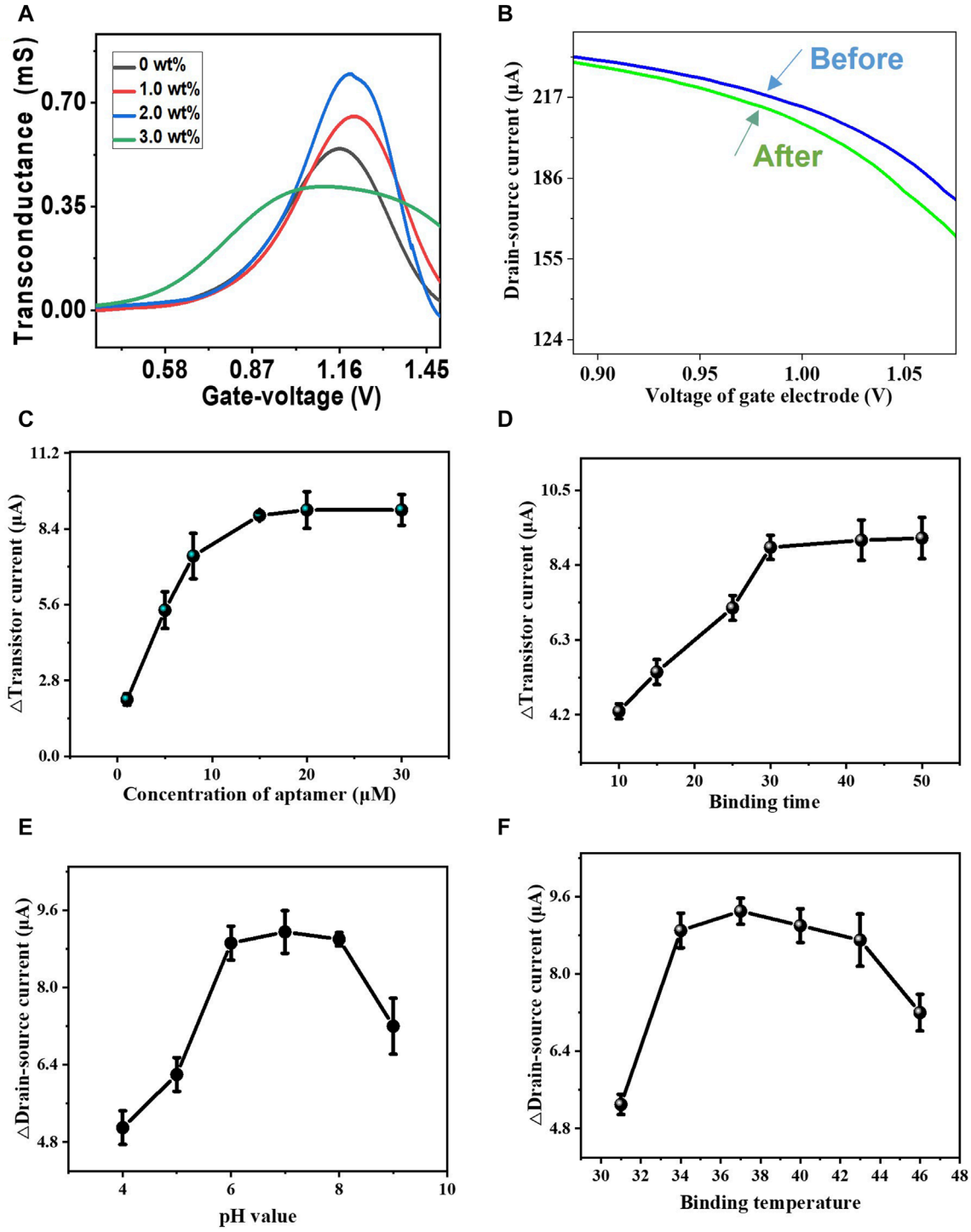

FIGURE 3
Optimizations of CM-OECATs. **(A)** Transconductance performance of CM-OECATs at different carbon nanotube concentrations, with a maximum of 0.801 mS at a carbon nanotube proportion of 2.0 wt%. **(B)** Transconductance curves before and after CM-OECATs binding with CEA. **(C)** Aptamer sensor concentration optimization for CM-OECATs, with the highest value at around 20 μM (9.12 ± 0.68 μA). **(D)** Incubation time optimization for CM-OECATs sensor, reaching the maximum at 30 min (8.91 ± 0.34 μA). **(E)** pH optimization for CM-OECATs, showing an upward then downward trend, reaching the highest value at pH = 7 (9.15 ± 0.44 μA). **(F)** Incubation temperature optimization for CM-OECATs, showing an upward then downward trend, reaching the maximum at around 37°C (9.23 ± 0.27 μA).

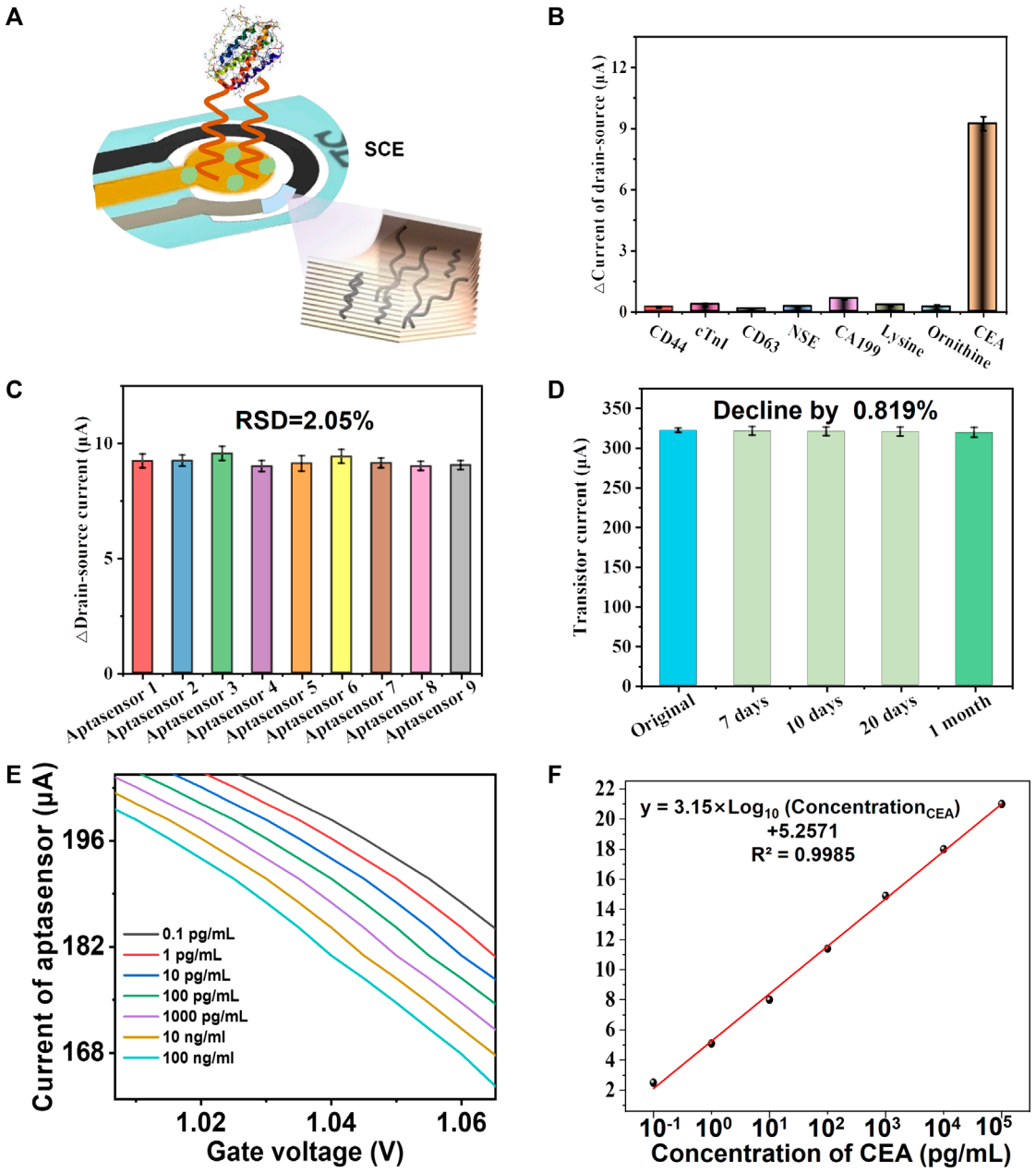

FIGURE 4
Validations of CM-OECATs. **(A)** Schematic diagram of CM-OECATs detection. **(B)** Specificity of CM-OECATs, showing a significantly higher signal response to CEA than other interfering substances. **(C)** Reproducibility of CM-OECATs, with an RSD value of only 2.05% for nine sensors. **(D)** Stability of CM-OECATs after 1 month, showing a decrease of only 0.819%. **(E)** Response of CM-OECATs to CEA in the range of 0.1 pg/mL to 100 ng/mL, and its corresponding **(F)** standard curve.

CM-OECATs reaches its maximum at 30 min (8.91 ± 0.34 μA, Figure 3D). For pH optimization, CM-OECATs pH exhibits an upward then downward trend, reaching its highest value at pH = 7 (9.15 ± 0.44 μA, Figure 3E). For temperature optimization, the incubation temperature of CM-OECATs shows an upward then downward trend, reaching its maximum at around 37°C (9.23 ± 0.27 μA, Figure 3F), coinciding with human body temperature and aligning with the parameters for antigen-aptamer binding. The optimization of the doping ratio and related parameters lays a beneficial foundation for the application of CM-OECATs in the next steps.

$$G_m = \frac{Wd}{L}\mu C^*(V_{th} - V_G) \quad (1)$$

where C^* is the volumetric capacitance, V_{th} is the threshold voltage, G_m is the transconductance, V_g is the gate voltage,μ is the mobility, W, D, L are the width, depth, length of the channel, respectively.

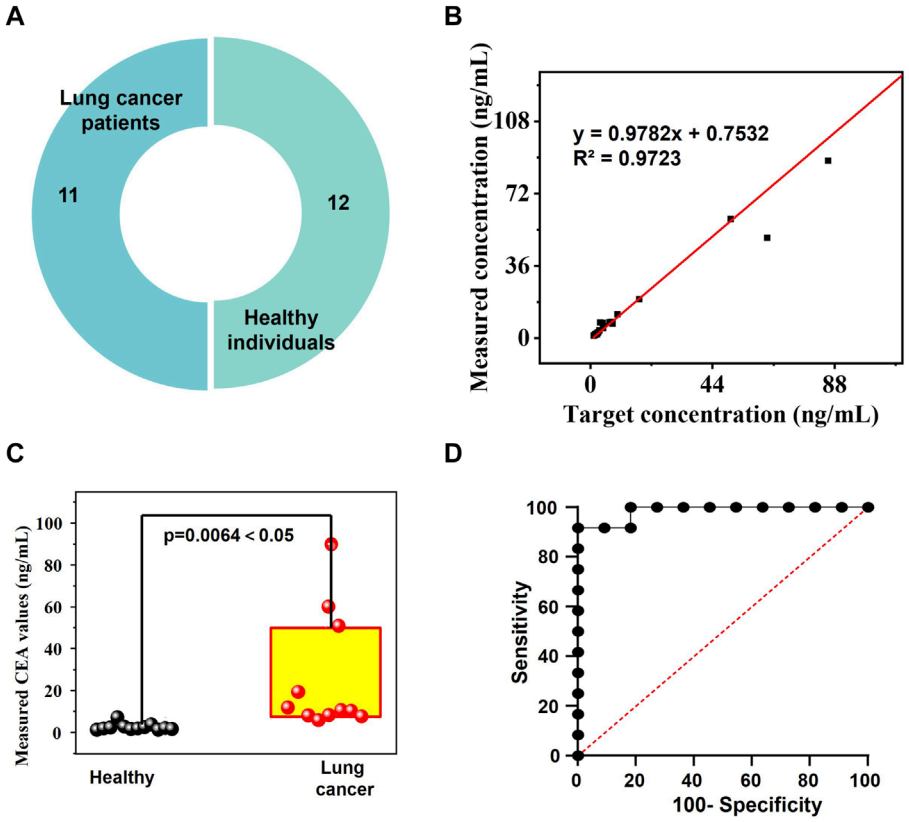

FIGURE 5
Clinical performance of CM-OECATs. **(A)** 11 lung cancer serum samples and 12 healthy control serum samples. **(B)** High correlation of values determined by CM-OECATs for 23 clinical samples with the target values (y = 0.9782x + 0.7532, R^2 = 0.9723). **(C)** *t*-test for 11 lung cancer serum samples and 12 healthy control serum samples by CM-OECATs, with a *p*-value of only 0.0064 < 0.05. **(D)** ROC curve analysis, showing effective discrimination (AUC = 0.9748, Specificity = 0.9565, Sensitivity = 0.9978).

3.3 CM-OECATs's specificity, reproducibility, stability, and standard calibration curve

The specificity, reproducibility, stability, and standard curve of the sensor are crucial for its clinical detection. Consequently, we evaluated the specificity of CM-OECATs by assessing their response to CEA in the presence of various interfering substances. CM-OECATs exhibited a signal response to CEA significantly higher than that of other interfering substances (Figures 4A, B). For reproducibility, we selected nine CM-OECATs sensors, with an RSD value of only 2.05%, indicating favorable reproducibility (Figure 4C). Regarding stability, CM-OECATs showed a decrease of only 0.819% after 1 month (Figure 4D), indicating good stability. Simultaneously, CM-OECATs demonstrated a wide range of CEA detection from 0.1 pg/mL to 100 ng/mL, with a detection limit of 0.0051 pg/mL (Figures 4E, F), showcasing performance that is either superior or equivalent to the current state-of-the-art literature. The above results demonstrate that CM-OECATs possess the required specificity, reproducibility, stability, and standard curve, providing a beneficial foundation for future clinical decisions.

3.4 CM-OECATs's clinical performance

We collected 11 lung cancer serum samples and 12 healthy control serum samples to assess the clinical performance of CM-OECATs (Figure 5A, Supplementary Table S2). Concurrently, CM-OECATs evaluated values for 23 clinical samples, showing a high correlation with the target values (Figure 5B, y = 0.9782x + 0.7532, R^2 = 0.9723), demonstrating the reliability of the CM-OECATs method The values obtained from CM-OECATs measurements exhibit a strong correlation with the target values in lung cancer patients (Supplementary Figure S1), demonstrating excellent performance. A similar correlation is observed in the case of healthy individuals (Supplementary Figure S2). Furthermore, CM-OECATs successfully passed a *t*-test for 11 lung cancer serum samples and 12 healthy control serum samples, with a *p*-value of only 0.0064 < 0.05 (Figure 5C). Moreover, employing ROC curve analysis, the sensor attained effective discrimination (AUC = 0.9748, Specificity = 0.9565, Sensitivity = 0.9978, Figure 5D). The analysis results of correlation, *t*-test, and ROC indicate that CM-OECATs exhibited favorable clinical performance.

4 Discussion

In selecting CNT-doped transition metal Carbide as the material for our organic electrochemical transistor biosensor, our rationale is primarily grounded in its capacity to augment the conductivity of semiconductor materials, complemented by its unique two-dimensional structure. The incorporation of carbon nanotubes (CNT) into the transition metal carbide, MXene, not only improves the electronic transport properties but also imparts unique characteristics owing to its two-dimensional nature. Opting for CNT-doped transition metal carbide paves the way for enhanced performance in the OECT sensor, fostering the hope that analogous structures will prove valuable in guiding the future design of organic electrochemical transistors. This strategic selection aligns with our objective to push the boundaries of sensor technology by leveraging advanced materials with enhanced electronic properties.

Furthermore, the utilization of CNT-doped MXene as the semiconductor material for CM-OECATs is highlighted, showcasing commendable performance in sensitivity, stability, reproducibility, and clinical sample detection. The merit of the sensor can be largely attributed to the synergistic effects of CNT doping, significantly enhancing the detection performance. This achievement not only validates our approach in utilizing CNT-Doped transition metal carbide but also provides insightful directions for future biosensor designs. The emphasis on enhancing detection capabilities becomes a cornerstone for the ongoing evolution of sensor technologies, inspiring novel strategies for the development of next-generation biosensors with improved sensing capabilities.

Looking forward, the future of clinical diagnostic sensors is envisioned to be more sensitive, user-friendly, and rapid. The imperative resides in developing new materials to enhance sensitivity and overall detection performance. The discussion underscores the crucial role of doped two-dimensional materials, particularly in opening new avenues for highly efficient diagnostic tools. By focusing on heightened sensitivity, convenience, and cost-effectiveness, we advocate for ongoing research in material science to drive innovation and contribute to the development of advanced clinical diagnostic sensors. The incorporation of doped two-dimensional materials emerges as a promising avenue for realizing efficient and accessible diagnostic methodologies in the future.

5 Conclusion

In this work, we have developed a novel material known as CNT-doped MXene, which has been incorporated in the construction of aptamer-based organic electrochemical transistor sensors, denoted as CM-OECATs. A rigorous validation procedure was used to evaluate the morphology and doping properties of CNT-doped MXene, revealing optimum doping efficiency at 2.0 wt% CNT, resulting in a notable transconductance of 0.801 ms. Systematic optimization of temperature, pH, aptamer concentration, and incubation time of CM-OECATs enabled a broad detection range ranging from 0.1 pg/mL to 100 ng/mL, with a remarkably low detection limit of 0.051 pg/mL. In particular, the biosensor demonstrated favourable stability (a decrease of 0.819%), specificity and reproducibility (RSD = 2.05%). The CM-OECATs demonstrated effective discrimination between 11 samples of lung cancer serum and 12 healthy controls in clinical sample analysis, showing remarkable performance metrics (AUC 0.9748, specificity 0.9565, and sensitivity 0.9978). *t*-test results from two sample batches yielded $0.0064 < 0.05$, highlighting the robust discrimination capability of CM-OECATs. In addition, the CM-OECATs demonstrated a strong clinical correlation between the 25 clinical specimens ($y = 0.9782x + 0.7532$, $R^2 = 0.9723$). To sum up, an aptamer-based organic electrochemical transistor sensor (CM-OECATs), which is constructed using CNT-doped MXene, holds great promise for future real-time clinical monitoring, indicating significant progress in efficient, cost-effective and highly sensitive detection technologies.

Data availability statement

The raw data supporting the conclusion of this article will be made available by the authors, without undue reservation.

Ethics statement

The studies involving humans were approved by the Ethics Committee of Shandong Chest Hospital. The studies were conducted in accordance with the local legislation and institutional requirements. The participants provided their written informed consent to participate in this study. The manuscript presents research on animals that do not require ethical approval for their study.

Author contributions

YZ: Formal Analysis, Methodology, Writing–original draft, Writing–review and editing. CS: Software, Writing–original draft. YT: Software, Writing–original draft. XL: Writing–original draft. DL: Data curation, Writing–original draft. AW: Methodology, Supervision, Writing–original draft. CW: Supervision, Writing–review and editing. XZ: Supervision, Writing–review and editing.

Funding

The author(s) declare financial support was received for the research, authorship, and/or publication of this article. This research was funded by Shandong Province Medical Health Science and Technology Development Plan Projects (202004021514, 202004021499, and 202004021501) and Science and Technology project of Sichuan Province (2023YFS0087).

Conflict of interest

The authors declare that the research was conducted in the absence of any commercial or financial relationships that could be construed as a potential conflict of interest.

Publisher's note

All claims expressed in this article are solely those of the authors and do not necessarily represent those of their affiliated organizations, or those of the publisher, the editors and the reviewers. Any product that may be evaluated in this article, or claim that may be made by its manufacturer, is not guaranteed or endorsed by the publisher.

Supplementary material

The Supplementary Material for this article can be found online at: https://www.frontiersin.org/articles/10.3389/fmats.2024.1354635/full#supplementary-material

References

Chen, X., Zheng, X., Yu, X., Li, X., Lin, Y., Lin, H., et al. (2023). Novel rapid coordination of ascorbic acid 2-phosphate and iron(III) as chromogenic substrate system based on Fe2O3 nanoparticle and application in immunoassay for the colorimetric detection of carcinoembryonic antigen. *Talanta* 258, 124414. doi:10.1016/j.talanta.2023.124414

Guo, K., Wustoni, S., Koklu, A., Díaz-Galicia, E., Moser, M., Hama, A., et al. (2021a). Rapid single-molecule detection of COVID-19 and MERS antigens via nanobody-functionalized organic electrochemical transistors. *Nat. Biomed. Eng.* 5, 666–677. doi:10.1038/s41551-021-00734-9

Guo, T., Lei, Y., Hu, X., Yang, G., Liang, J., Huang, Q., et al. (2022). Hydrothermal synthesis of MXene-MoS2 composites for highly efficient removal of pesticides. *Appl. Surf. Sci.* 588, 152597. doi:10.1016/j.apsusc.2022.152597

Guo, Y., Zhang, D., Yang, Y., Wang, Y., Bai, Z., Chu, P. K., et al. (2021b). MXene-encapsulated hollow Fe3O4nanochains embedded in N-doped carbon nanofibers with dual electronic pathways as flexible anodes for high-performance Li-ion batteries. *Nanoscale* 13, 4624–4633. doi:10.1039/d0nr09228b

Huang, H., Li, L., Luo, W., Yang, Y., Ni, Y., Song, T., et al. (2022). Lymphocyte percentage as a valuable predictor of prognosis in lung cancer. *J. Cell. Mol. Med.* 26, 1918–1931. doi:10.1111/jcmm.17214

Hui, X., Zhao, R., Zhang, P., Li, C., Wang, C., and Yin, L. (2019). Low-temperature reduction strategy synthesized Si/Ti3C2 MXene composite anodes for high-performance Li-ion batteries. *Adv. Energy Mat.* 9, 201901065. doi:10.1002/aenm.201901065

Kim, J., Jang, M., Jeong, G., Yu, S., Park, J., Lee, Y., et al. (2021). MXene-enhanced β-phase crystallization in ferroelectric porous composites for highly-sensitive dynamic force sensors. *Nano Energy* 89, 106409. doi:10.1016/j.nanoen.2021.106409

Li, H., Dauphin-Ducharme, P., Arroyo-Currás, N., Tran, C. H., Vieira, P. A., Li, S., et al. (2017). A biomimetic phosphatidylcholine-terminated monolayer greatly improves the *in vivo* performance of electrochemical aptamer-based sensors. *Angew. Chem.* 129, 7600–7603. doi:10.1002/ange.201700748

López Barreiro, D., Martín-Moldes, Z., Yeo, J., Shen, S., Hawker, M. J., Martin-Martinez, F. J., et al. (2019). Conductive silk-based composites using biobased carbon materials. *Adv. Mat.* 31, e1904720. doi:10.1002/adma.201904720

Meirinho, S. G., Dias, L. G., Peres, A. M., and Rodrigues, L. R. (2017). Electrochemical aptasensor for human osteopontin detection using a DNA aptamer selected by SELEX. *Anal. Chim. Acta* 987, 25–37. doi:10.1016/j.aca.2017.07.071

Mojtabavi, M., Vahidmohammadi, A., Liang, W., Beidaghi, M., and Wanunu, M. (2019). Single-Molecule sensing using nanopores in two-dimensional transition metal carbide (MXene) membranes. *ACS Nano* 13, 3042–3053. doi:10.1021/acsnano.8b08017

Moser, M., Hidalgo, T. C., Surgailis, J., Gladisch, J., Ghosh, S., Sheelamanthula, R., et al. (2020). Side chain redistribution as a strategy to boost organic electrochemical transistor performance and stability. *Adv. Mat.* 32, e2002748. doi:10.1002/adma.202002748

Paniagua, G., Villalonga, A., Eguílaz, M., Vegas, B., Parrado, C., Rivas, G., et al. (2019). Amperometric aptasensor for carcinoembryonic antigen based on the use of bifunctionalized Janus nanoparticles as biorecognition-signaling element. *Anal. Chim. Acta* 1061, 84–91. doi:10.1016/j.aca.2019.02.015

Qin, L., Tao, Q., El Ghazaly, A., Fernandez-Rodriguez, J., Persson, P. O. Å., Rosen, J., et al. (2018). High-performance ultrathin flexible solid-state supercapacitors based on solution processable Mo1.33C MXene and PEDOT:PSS. *Adv. Funct. Mat.* 28, 1–8. doi:10.1002/adfm.201703808

Qiu, Z., Shu, J., Liu, J., and Tang, D. (2019). Dual-Channel photoelectrochemical ratiometric aptasensor with up-converting nanocrystals using spatial-resolved technique on homemade 3D printed device. *Anal. Chem.* 91, 1260–1268. doi:10.1021/acs.analchem.8b05455

Ramuz, M., Hama, A., Rivnay, J., Leleux, P., and Owens, R. M. (2015). Monitoring of cell layer coverage and differentiation with the organic electrochemical transistor. *J. Mat. Chem. B* 3, 5971–5977. doi:10.1039/c5tb00922g

Si, Z., Xie, B., Chen, Z., Tang, C., Li, T., and Yang, M. (2017). Electrochemical aptasensor for the cancer biomarker CEA based on aptamer induced current due to formation of molybdophosphate. *Microchim. Acta* 184, 3215–3221. doi:10.1007/s00604-017-2338-5

Spyropoulos, G. D., Gelinas, J. N., and Khodagholy, D. (2020). Internal ion-gated organic electrochemical transistor: a building block for integrated bioelectronics. *Sci. Adv.* 5, eaau7378. doi:10.1126/SCIADV.AAU7378

Sung, H., Ferlay, J., Siegel, R. L., Laversanne, M., Soerjomataram, I., Jemal, A., et al. (2021). Global cancer statistics 2020: GLOBOCAN estimates of incidence and mortality worldwide for 36 cancers in 185 countries. *Ca. Cancer J. Clin.* 71, 209–249. doi:10.3322/caac.21660

Wang, C., Liu, L., and Zhao, Q. (2020). Low temperature greatly enhancing responses of aptamer electrochemical sensor for aflatoxin B1 using aptamer with short stem. *ACS Sensors* 5, 3246–3253. doi:10.1021/acssensors.0c01572

Wang, S., Yu, H., Gan, Y., Wu, Z., Li, E., Li, X., et al. (2022). Mining whole-lung information by artificial intelligence for predicting EGFR genotype and targeted therapy response in lung cancer: a multicohort study. *Lancet Digit. heal.* 4, e309–e319. doi:10.1016/S2589-7500(22)00024-3

Wang, Y., Luo, J., Liu, J., Sun, S., Xiong, Y., Ma, Y., et al. (2019). Label-free microfluidic paper-based electrochemical aptasensor for ultrasensitive and simultaneous multiplexed detection of cancer biomarkers. *Biosens. Bioelectron.* 136, 84–90. doi:10.1016/j.bios.2019.04.032

Wang, Z., Wang, F., Hermawan, A., Asakura, Y., Hasegawa, T., Kumagai, H., et al. (2021). SnO-SnO2 modified two-dimensional MXene Ti3C2T for acetone gas sensor working at room temperature. *J. Mat. Sci. Technol.* 73, 128–138. doi:10.1016/j.jmst.2020.07.040

Wee, G., Larsson, O., Srinivasan, M., Berggren, M., Crispin, X., and Mhaisalkar, S. (2010). Effect of the ionic conductivity on the performance of polyelectrolyte-based supercapacitors. *Adv. Funct. Mat.* 20, 4344–4350. doi:10.1002/adfm.201001096

Wei, S., Fu, Y., Liu, M., Yue, H., Park, S., Lee, Y. H., et al. (2022). Dual-phase MoS2/MXene/CNT ternary nanohybrids for efficient electrocatalytic hydrogen evolution. *npj 2D Mat. Appl.* 6, 25–644. doi:10.1038/s41699-022-00300-0

Wu, X., Surendran, A., Ko, J., Filonik, O., Herzig, E. M., Müller-Buschbaum, P., et al. (2019). Ionic-liquid doping enables high transconductance, fast response time, and high ion sensitivity in organic electrochemical transistors. *Adv. Mat.* 31, e1805544. doi:10.1002/adma.201805544

Yang, G., Xiao, Z., Tang, C., Deng, Y., Huang, H., and He, Z. (2019). Recent advances in biosensor for detection of lung cancer biomarkers. *Biosens. Bioelectron.* 141, 111416. doi:10.1016/j.bios.2019.111416

Zahed, M. A., Sharifuzzaman, M., Yoon, H., Asaduzzaman, M., Kim, D. K., Jeong, S., et al. (2022). A nanoporous carbon-MXene heterostructured nanocomposite-based epidermal patch for real-time biopotentials and sweat glucose monitoring. *Adv. Funct. Mat.* 32, 202208344. doi:10.1002/adfm.202208344

Zamzami, M. A., Rabbani, G., Ahmad, A., Basalah, A. A., Al-Sabban, W. H., Nate Ahn, S., et al. (2022). Carbon nanotube field-effect transistor (CNT-FET)-based biosensor for rapid detection of SARS-CoV-2 (COVID-19) surface spike protein S1. *Bioelectrochemistry* 143, 107982. doi:10.1016/j.bioelechem.2021.107982

Zhang, Y. Z., Wang, Y., Jiang, Q., El-Demellawi, J. K., Kim, H., and Alshareef, H. N. (2020). MXene printing and patterned coating for device applications. *Adv. Mat.* 32, e1908486. doi:10.1002/adma.201908486